Bioorganic & Medicinal Chemistry Letters 24 (2014) 1565–1570

Contents lists available at ScienceDirect

Bioorganic & Medicinal Chemistry Letters

journal homepage: www.elsevier.com/locate/bmcl

Inhibition of cellular proliferation and induction of apoptosis in human lung adenocarcinoma A549 cells by T-type calcium channel antagonist

Doo Li Choi [a], Sun Jeong Jang [a], Sehyeon Cho [a], Hye-Eun Choi [b], Hong-Kun Rim [b], Kyung-Tae Lee [b], Jae Yeol Lee [a,*]

[a] Research Institute for Basic Sciences and Department of Chemistry, College of Sciences, Kyung Hee University, Seoul 130-701, Republic of Korea
[b] Department of Life and Nanopharmaceutical Science, College of Pharmacy, Kyung Hee University, Seoul 130-701, Republic of Korea

ARTICLE INFO

Article history:
Received 11 November 2013
Revised 15 January 2014
Accepted 24 January 2014
Available online 3 February 2014

Keywords:
T-type calcium channel
Antagonist
Human lung adenocarcinoma (A549) cells
Pancreatic cancer (MiaPaCa2) cells
Apoptosis
Cell cycle arrest
Caspases

ABSTRACT

The anti-proliferative and apoptotic activities of new T-type calcium channel antagonist, **6e** (**BK10040**) on human lung adenocarcinoma A549 cells were investigated. The MTT assay results indicated that **BK10040** was cytotoxic against human lung adenocarcinoma (A549) and pancreatic cancer (MiaPaCa2) cells in a dose-dependent manner with IC_{50} of 2.25 and 0.93 μM, respectively, which is ca. 2-fold more potent than lead compound **KYS05090** despite of its decreased T-type calcium channel blockade. As a mode of action for cytotoxic effect of **BK10040** on lung cancer (A549) cells, this cancer cell death was found to have the typical features of apoptosis, as evidenced by the accumulation of positive cells for annexin V. In addition, **BK10040** triggered the activations of caspases 3 and 9, and the cleavages of poly (ADP-ribose) polymerase (PARP). Moreover, the treatment with z-VAD-fmk (a broad spectrum caspase inhibitor) significantly prevented **BK10040**-induced apoptosis. Based on these results, **BK10040** may be used as a potential therapeutic agent for human lung cancer via the potent apoptotic activity.

Calcium plays a key role in intracellular signaling and controls many different cell processes such as proliferation, differentiation, growth, cell death and apoptosis.[1,2] Thus, alterations in calcium signaling can cause defects in cell growth and are associated with certain types of cancer.[3,4] A number of research groups have suggested a potential role for voltage-activated Ca^{2+} channels, in particular T-type (Ca_v3), in the regulation of tumor growth and progression.[5–9] This T-type Ca^{2+} channel family (Ca_v3) contains three members: $Ca_v3.1$ (α_{1G}), $Ca_v3.2$ (α_{1H}) and $Ca_v3.3$ (α_{1I}).[10] There is a growing body of evidence that some of T-type Ca^{2+} channels are abnormally expressed in cancerous cells compared to normal cells and thus the blockade of these channels may reduce cell proliferation in addition to inducing apoptosis in cancer cells.[11–15]

Lung cancer is the most common malignant tumor in the world. Non-small cell lung cancer (NSCLC) is the majority of lung cancer, approximately 80% of total malignancies, with a 5-year survival of only 15%. The other 20% of total lung cancer is small cell lung cancer (SCLC).[16] In our previous papers, our group have reported that 3,4-dihydroquinazoline derivatives exhibited in vitro and in vivo anti-proliferative effects against lung cancer (A549) cells via T-type calcium channel blockade.[17–20] In an effort to improve anti-proliferative activity of lead compound **KYS050590** as 3,4-dihydroquinazoline derivative, we incorporated bioisosteres into our further optimization process because this strategy has been frequently used for such a purpose in conventional medicinal chemistry.[21] Accordingly, the modification of three parts (P-1, P-2, and P-3 part) in **KYS05090** led to new eight 3,4-dihydroquinazoline derivatives as shown in Figure 1 and Table 1. Among these compounds, **6e** (**BK10040**) was found to be more potent than **KYS05090** against human lung adenocarcinoma (A549) and pancreatic cancer (MiaPaCa2) cells. Compound **6e** (**BK10040**) was obtained by the replacement of *N*,*N*′,*N*′-trimethyl-1,5-pentanediamine chain at P-1 part and biphenyl ring at P-2 part with 4-[2-(dimethylamino)ethyl]piperazine ring and *p*-cyclohexylphenyl ring, respectively, as shown in Figure 1. Herein we focus on how **BK10040** can contribute to anti-proliferative activity in human lung adenocarcinoma (A549) cells via T-type calcium channel blockade.

We have synthesized new 3,4-dihydroquinazoline derivatives through the modification of P-1, P-2, and P-3 parts by the same procedure as described previously by our group as outlined in Schemes 1 and 2.[17–20] The reduction of *trans*-2-nitrocinnamate **1** with activated Zn and NH_4Cl in MeOH afforded *trans*-2-aminocinnamate **2**, followed by an addition of commercially available or

* Corresponding author. Tel.: +82 2 961 0726; fax: +82 2 966 3701.
E-mail address: ljy@khu.ac.kr (J.Y. Lee).

http://dx.doi.org/10.1016/j.bmcl.2014.01.071
0960-894X/

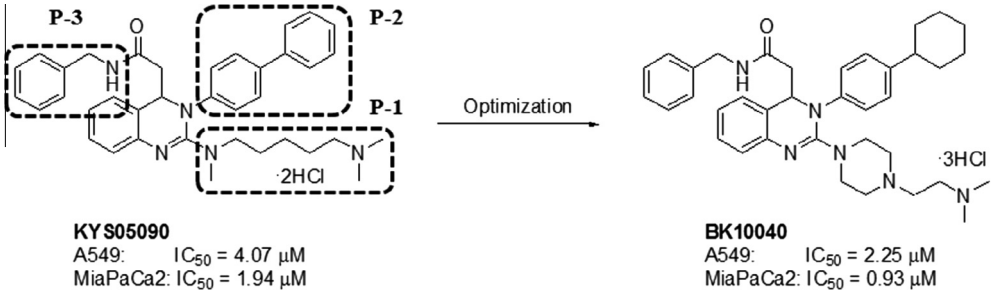

Figure 1. Discovery of new 3,4-dihydroquinazoline derivative **6e** (**BK10040**) via a modification of substituents of lead compound **KYS05090**.

Table 1
T-type Ca^{2+} channel blocking effect and anti-proliferative effect against lung (A549) and pancreatic (MiaPaCa2) cancer cells of T-type Ca^{2+} channel antagonists

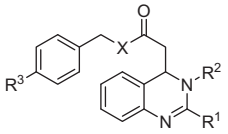

Entry	R^1	R^2	R^3	X	Calcium channel blockade [T-type: $Ca_v3.1$ (α_{1G})][a]		Cytotoxicity: IC_{50} (μM)[c]	
					% Inhibition (@ 1 μM)[b]	(IC_{50}: μM)[b]	A549	MiaPaCa2
KYS05090	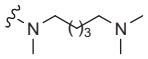	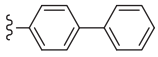	H	NH	76.6 ± 0.7	0.26 ± 0.01	4.07	1.94
5b	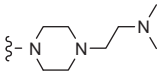	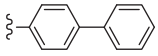	H	O	46.4 ± 4.7	1.81 ± 0.21	4.29	2.70
6a	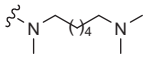	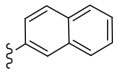	H	NH	26.4 ± 2.8	ND[d]	5.44	2.54
6b	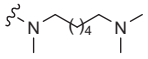	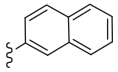	OMe	NH	55.2 ± 2.3	0.73 ± 0.07	6.65	3.99
6c	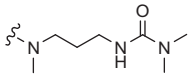	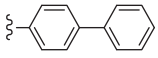	F	NH	53.5 ± 1.9	0.60 ± 0.06	14.95	7.43
6d	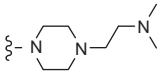	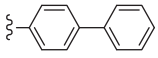	NO_2	NH	38.1 ± 1.5	ND[d]	4.69	2.18
6e (**BK10040**)	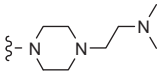	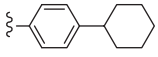	H	NH	53.2 ± 1.5	1.04 ± 0.10	2.25	0.93
6f	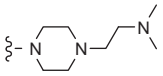	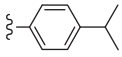	H	NH	39.2 ± 1.6	ND[d]	7.57	3.02
8	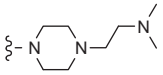	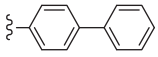	$N(SO_2Me)_2$	NH	64.3 ± 3.5	0.52 ± 0.08	20.70	16.11
Mibefrail	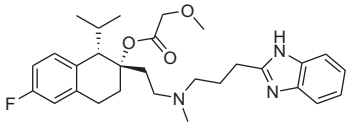				55.1 ± 1.1	0.56 ± 0.11	24.8	18.4

[a] T-type calcium channel (α_{1G}) expressed on HEK293 cell.
[b] Value was determined from dose–response curve and obtained from three independent experiments.
[c] MTT assay.
[d] ND: not determined when less than 40% inhibition at 1 μM.

in situ generated isocyanate from the reaction of the corresponding carboxylic acid and diphenyl phosphorazidate (DPPA) in the presence of TEA produced urea compound **3**. The amine chains for R^2 substituent were synthesized as outlined in Scheme 2: *N*,*N*′,*N*′-trimethyl-1,6-hexanediamine (**13**) was prepared according to the previously reported method.[19] For 3-(*N*,*N*-dimethylureidopropyl)-1-methylamine **17**, selective mono-protection of secondary amine in **14** with di-*tert*-butyl dicarbonate and subsequent *N*-acylation with dimethylcarbamoyl chloride afforded compound **16**, which was treated with 3 N HCl to give the target compound **17**. The dehydration of **3** with $Ph_3P{\cdot}Br_2$ and Et_3N provided carbodiimide **4**, which was coupled with commercially available piperazine ring or the above amine chain (**13** or **17**) to afford the 3,4-dihydroquinazoline ester derivative **5a**–**b**, respectively. The treatment of methyl ester **5a** (R = Me) with *p*-R^3-benzylamine and 1,5,7-triazabicyclo[4.4.0]dec-5-ene (TBD) as a catalyst under solvent-free

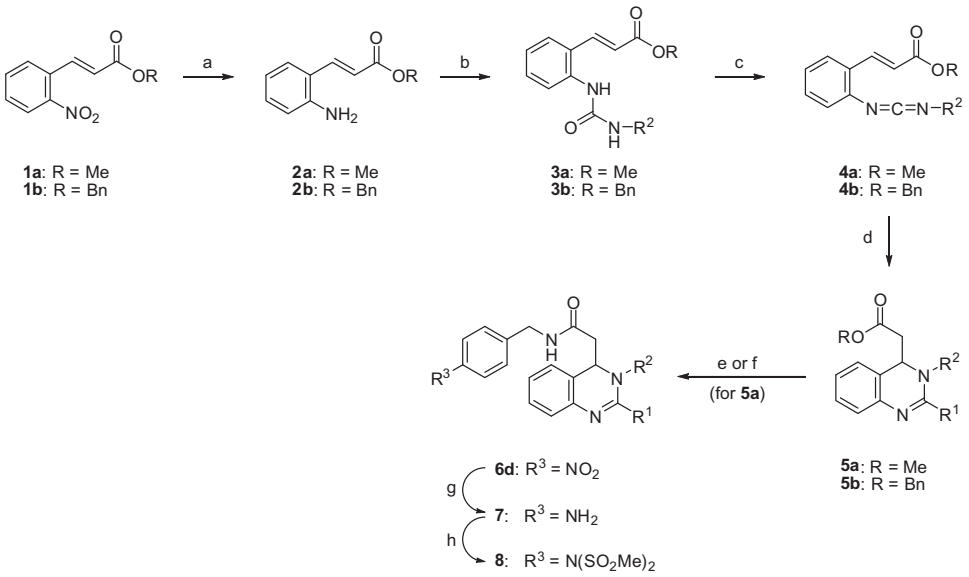

Scheme 1. Reagents and conditions:(a) Zn, NH_4Cl, MeOH, reflux, 12 h, 95–96%; (b) R^2-CO_2H, DPPA, Et_3N /or R^2-NCO, toluene, rt to 100 °C, 12 h, 55–79%; (c) $Ph_3P{\cdot}Br_2$, Et_3N, CH_2Cl_2, 0 °C, 12 h, 64–81%; (d) compound **13** or **17** in Scheme 2 or 4-[2-(dimethylamino)ethyl]piperazine, toluene, rt, 3 h, 44–97%; (e) *p*-R^3-$BnNH_2$, TBD, rt, 3 h, 61–89%; (f) (i) $LiOH{\cdot}H_2O$, THF–H_2O (1:1), 70 °C, 12 h, quantitative, (ii) EDC, HOBt, *p*-NO_2-$BnNH_2$, THF–CH_2Cl_2 (1:1), 0 °C to rt, 54% (for **6d**); (g) H_2, 5% Pd/C, MeOH, rt, 48 h, 74%; (h) Me_2SO_2Cl (1 equiv), TEA, CH_2Cl_2, rt, 1 h, 67%.

condition afforded directly the corresponding 3,4-dihydroquinazoline amide derivative **6**, respectively. In the case of only *p*-nitrobenzyl amide **6d**, the methyl ester **5a** was hydrolyzed with LiOH to provide the free carboxylic compound in quantitative yield. This acid compound was coupled with *p*-nitrobenzylamine by using EDC and HOBt to give the *p*-nitrobenzylamide **6d**, followed by hydrogenation with 5% Pd/C afforded *p*-aminobenzyl amide **7**. The coupling of **7** with 1 equiv of methansulfonyl chloride in the presence of Et3N afforded unexpectedly bis(methanesulfonyl)amino compound **8**. Finally, a series of **6a–f** were prepared as HCl salt by treatment with concd HCl in EtOAc solution.

The channel blocking activity for new 3,4-dihydroquinazoline derivatives was evaluated against T-type channel $Ca_v3.1$ (α_{1G}) expressed on HEK293 cell at 1 μM concentration by whole cell patch-clamp methods.[22] For only compounds showing more than 40% inhibition value, the molar concentrations (IC_{50}) of compounds required to produce 50% inhibition of α_{1G} T-type currents were determined from fitting raw data into dose–response curves. All derivatives were evaluated for anti-proliferative activity against human lung adenocarcinoma (A549) and pancreatic cancer (MiaPaCa2) cells using MTT assay.[23] Both assay results for the inhibition of calcium influx and the cytotoxicity on human cancer cells were summarized in Table 1 together with those of mibefradil and **KYS05090** as positive controls.

With respect to T-type channel blocking effect, all trials of replacement of P-1 and/or P-2 and/or P-3 part in **KYS05090** with various substituents led to a decrease in potency (both % inhibitions at 1 μM and IC_{50} values) and four analogs (**5**, **6a**, **6d**, and **6f**) was particularly far less potent than **KYS05090**, indicating the importance of the appropriate methylene unit ($n = 3$) of diamine chain at P-1 part, the biphenyl ring at P-2 part, and the amide bond at P-3 part for potent T-type channel blockade. This assay result was practically consistent with our previously extensive SAR studies on a variety of 3,4-dihydroquinazoline derivatives for T-type Ca^{2+} channel blockade.[17–20]

With respect to cytotoxic effect on both cancer cells, first of all, all new analogs disclosed a broad spectrum of cytotoxicity with IC_{50} values of 0.93 into 20.78 μM irrespective of a degree of T-type

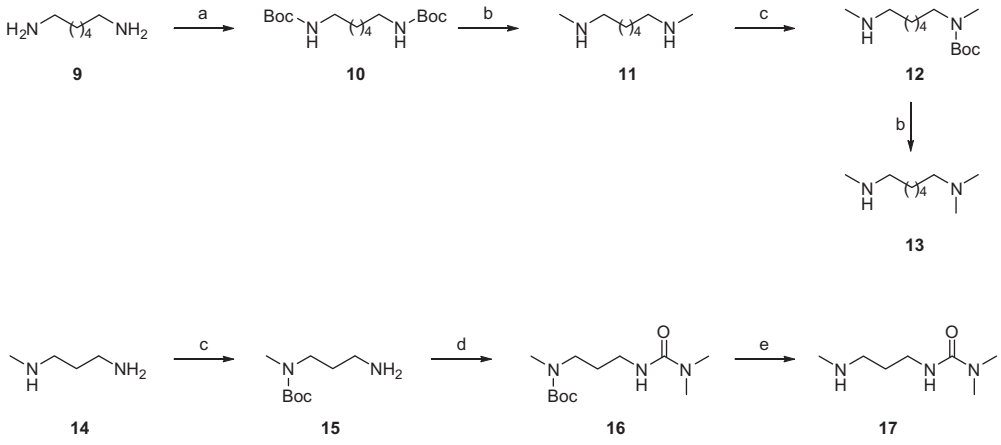

Scheme 2. Reagents and conditions: (a) $(Boc)_2O$, MeOH, rt, 1 h, 91%; (b) $LiAlH_4$, THF, reflux, 12 h, 96% for **11** and 50% for **13**; (c) $(Boc)_2O$, MeOH, concd HCl, 0 °C to rt, 3 h, 33% for **12** and 23% for **15**; (d) dimethylcarbamoyl chloride, CH_2Cl_2, −10 °C, 4 h, 75%; (e) 3 N HCl, MeOH, rt, quantitative.

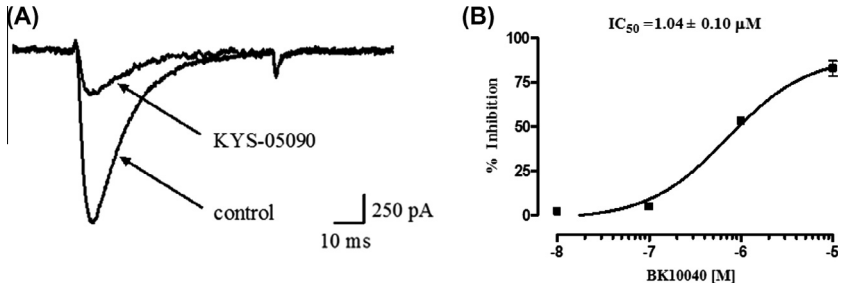

Figure 2. Inhibition of T-type Ca^{2+} channel current by **KYS05090** and **6e** (**BK10040**) as assessed by manual electrophysiology. Voltage protocol is that T-type $Ca_v3.1$ currents were evoked every 15 s by a 50 ms depolarizing voltage step from −100 mV to −30 mV. (A) Representative current traces illustrating the inhibition of T-type Ca^{2+} channel by 18 μM **KYS05090**. (B) Dose–response curve for **BK10040** yielded an IC_{50} value.

Table 2
The cell cycle phase distribution of human lung adenocarcinoma (A549) cells by T-type Ca^{2+} channel antagonists

Compound	Cell cycle phase (%) in A549[a]							
	For 24 h				For 48 h			
	Sub-G_1	G_0/G_1	S	G_2/M	Sub-G_1	G_0/G_1	S	G_2/M
KYS05090	55.3	33.6	8.8	2.2	98.1	1.2	0.6	0.1
6e (BK10040)	15.8	55.4	12.8	16.0	77.8	15.7	4.6	1.9
Mibefradil[b]	9.6	66.1	10.9	13.4	10.0	66.8	12.0	11.2
Control[c]	7.8	53.1	17.6	21.6	4.9	57.8	12.0	25.4

[a] Effect of each compound @ 5 μM on the cell cycle progression of A549 cells.
[b] Effect of mibefradil @ 10 μM on the cell cycle progression of A549 cells.
[c] Untreated A549 cells.

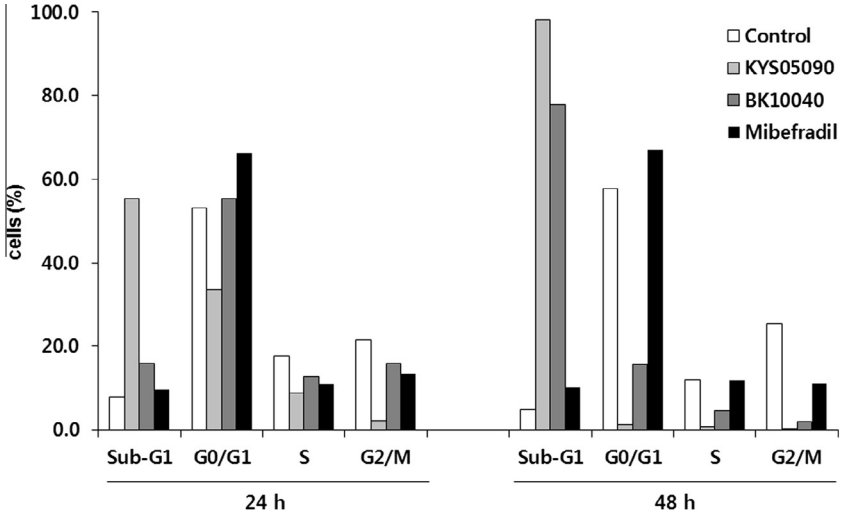

Figure 3. The effect of T-type Ca^{2+} channel antagonist on the cell cycle arrest in A549 lung cancer cells. A549 cells were treated with 5 μM concentration of each antagonist for 24 or 48 h, respectively. Cell cycle phases were detected by FACS.

channel blockade, as shown in Table 1. Interestingly, all derivatives as well as **KYS05090** were about 2-fold more potent against pancreatic (MiaPaCa2) cancer cells than against lung (A549) cancer cells. Among them, new derivative **6a** containing 1,6-diamine at R^1/a naphthalene ring at R^2, **6d** containing a piperazine ring at R^1/a nitro group at R^3, and **6f** containing a piperazine ring at R^1/a *p*-isopropylphenyl ring at R^2 exhibited appropriate activities with IC_{50} values of 5.44, 4.69 and 7.57 μM, respectively, despite of lower channel blocking effects (>40% inhibitions at 1 μM). On the contrary, new derivative **6c** containing ω-ureido group at R^1/ fluoro atom at R^3, and **8** containing a piperazine ring at R^1/*p*-bis(methansulfone)amido group at R^3 showed less activities with IC_{50} values of 14.95 and 20.70 μM, respectively, despite of potent channel blocking effects comparable to that of **KYS05090**. Finally, it should be noticed that **6e** (**BK10040**) possessing a piperazine ring at R^1 and a *p*-cyclohexylphenyl ring at R^2 was ca. 2-fold and 4-fold less potent (IC_{50} = 1.04 ± 0.10 μM) than mibefradil and **KYS05090**, respectively, for T-type Ca^{2+} channel ($Ca_v3.1$) blockade as shown in Figure 2. Despite of this relatively less degree of T-type channel blockade, however, **6e** (**BK10040**) showed ca. 2-fold more potency (IC_{50} = 2.25 and 0.93 μM) against both human cancer cells than **KYS05090**.

In order to investigate this discordance between T-type Ca^{2+} channel blocking effect and anti-proliferative effect, therefore, the effect of **6e** (**BK10040**) on cell cycle progression of A549 cells was performed using flow cytometry (FACS)[24] together with those of mibefradil and **KYS05090** as positive controls. Flow cytometry-generated cell cycle phase distribution revealed that A549 cells

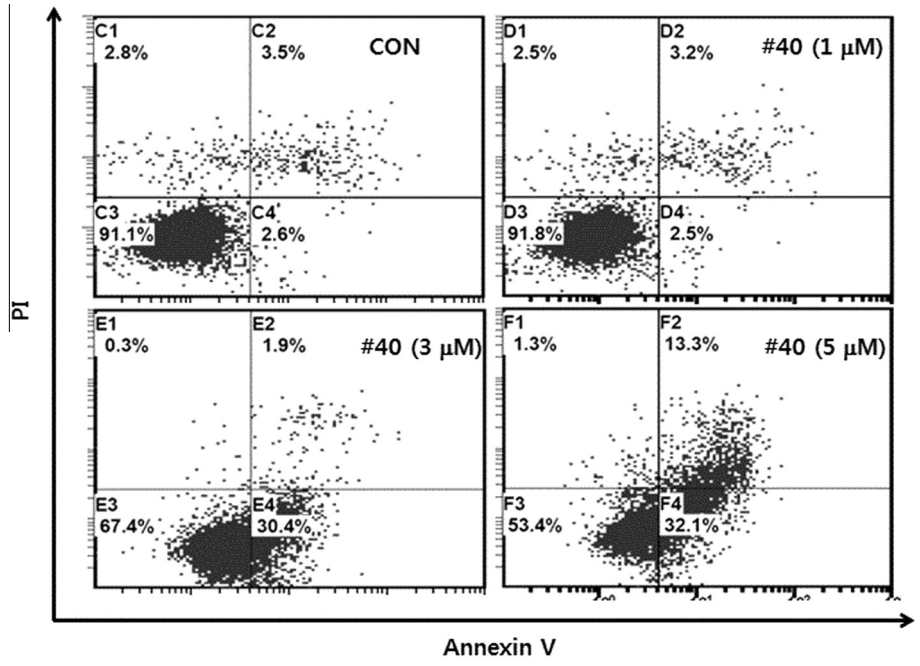

Figure 4. Compound **6e** (**BK10040**) induces apoptosis in A549 lung cancer cells. A549 cells were stained with Annexin V (FITC) and propidium iodide (PI) after treatment with **6e** (**BK10040**). Fluorescence-activated cell sorting analysis of A549 cells at 24 h following treatment with 0, 1, 3, and 5 μM **6e** (**BK10040**) (C, D, E, F, respectively). Percentage of each 2 and 4 area represents Annexin V-positive/PI-negative (early apoptotic) and Annexin V-positive/PI-positive cells (apoptotic), respectively.

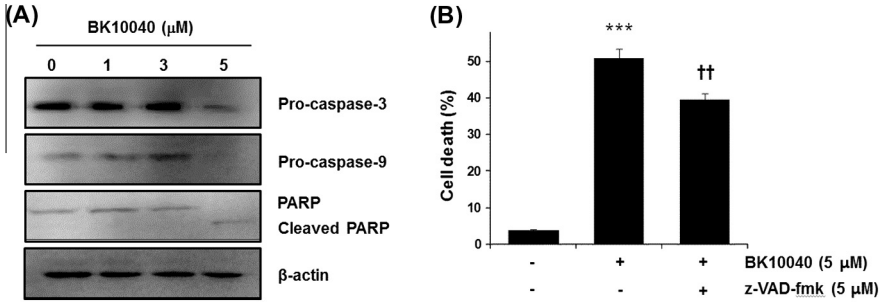

Figure 5. (A) **6e** (**BK10040**) alters pro-caspase-3, -9 and PAPR levels in A549 lung cancer cells. Western blot analysis of cells treated without or with **6e** (**BK10040**) (1, 3 or 5 μM). **(B)** Cell death treated with 5 μM **6e** (**BK10040**) in the absence or presence of 5 μM z-VAD-fmk.

treated with each compound for 24 or 48 h harvest exhibited a distribution of cell cycle phase as shown in Table 2 and Figure 3. The very high percentage of sub-G_1 phase for **KYS05090-**treatment indicated the A549 cell death for 24 or 48 h harvest due to its inherent strong cytotoxicity as well as T-type channel blockade. In the case of **6e** (**BK10040**)-treatment for 24 h, A549 cells showed a little increment in the sub-G_1 phase, and a little reduction in S and G_2/M phase of the cell cycle compared to those of untreated control. After 48 h, the percentage of cells in the sub-G_1 phase was significantly increased and the G_0/G_1 phase was significantly decreased in response to **6e** (**BK10040**)-treatment comparable to that of **KYS05090**-treated cells. Therefore, T-type Ca^{2+} channel blockade-induced sub-G_1 phase (cell death) increment may be one of possible mechanisms of anti-proliferative activity for **6e** (**BK10040**), which is consistent with the reported literatures.[25–28]

Generally, the sub-G_1 phase (cell death) may be related with the induction of apoptosis or necrosis in A549 cells via T-type Ca^{2+} channel blockade. Thus, fluorescence-activated cell sorting analysis was performed to identify the possibility of induction of apoptosis in A549 cell when treated with **6e** (**BK10040**). FACS analysis of Annexin V-FITC and PI stained A549 cells was used to determine the percentage of viable and apoptotic cells following treatment with **6e** (**BK10040**) for 24 h.[29] As shown in Figure 4, a dose-dependent effect of **6e** (**BK10040**) in inducing apoptosis in A549 cells was observed. The percentage sum of early apoptotic cells (Annexin V-positive/PI-negative) and late apoptotic cells (Annexin V-positive/PI-positive) was 6.1% for control, 5.7% for 1 μM, 32.3% for 3 μM and 45.4% for 5 μM of **6e** (**BK10040**), respectively.

The induction of apoptosis essentially needs the activation of caspases as a group of intracellular proteases, which are responsible for planning the cell into apoptotic bodies during apoptosis.[30–33] Caspases are present as inactive proenzymes that are activated by proteolytic cleavage.[34] In particular, caspases-3, -8, and -9 are situated at pivotal junctions in apoptosis pathways.[35–37] Therefore, the effect of **6e** (**BK10040**) on the expression of proteins related to apoptosis was tested. As shown in Figure 5(A), treatment of A549 cells with 5 μM **6e** (**BK10040**) for 24 h significantly reduced the expression of pro-caspase-3 and -9, indicating the potential activation of both of caspase-3 and -9 via proteolytic cleavage. In addition, increased cleavage of PARP protein was seen after a 24 h exposure to 5 μM **6e** (**BK10040**). To further confirm the involvement of caspases in **6e** (**BK10040**)-induced apoptosis, z-VAD-fmk (a broad spectrum caspase inhibitor) was used at concentrations that completely blocked the activations of caspases.[38] As shown

in Figure 5(B), z-VAD-fmk significantly suppressed **6e** (**BK10040**)-induced apoptosis from 50% to 39%, indicating that **6e** (**BK10040**) induced apoptosis is partly dependent on the activation of caspases. Taken together, these biological results demonstrate that **6e** (**BK10040**) displayed an induction of apoptosis in A549 cells via caspase-3 and caspase-9-dependent pathway triggered by T-type Ca^{2+} channel blockade.

In conclusion, new synthetic 3,4-dihydroquinazoline derivative **6e** (**BK10040**) was found to be more potent than lead compound **KYS05090** against human lung adenocarcinoma (A549) and pancreatic cancer (MiaPaCa2) cells, whereas it showed the decreased effect of T-type Ca^{2+} channel blockade compared to that of **KYS05090**. As a study on mode of action for cytotoxic effect on A549 cells, this compound was found to induce the death of human lung cancer (A549) cell via T-type Ca^{2+} channel blockade based on the increased cell cycle phase at sub-G_1 phase 48 h after treatment. The induction of apoptosis as a cell death pathway is also found to be mediated through the activation of both of caspase-3 and -9. Thus, **6e** (**BK10040**)[39] was decided to further evaluate in vivo efficacy using xenograft animal model in order to identify a potential therapeutic agent for human lung cancer. In vivo experimental as well as pharmacokinetics profiles are in progress and will be announced in the future.

Acknowledgment

This work was supported by a Grant from the Kyung Hee University in 2012 (KHU-20120770).

Supplementary data

Supplementary data associated with this article can be found, in the online version, at http://dx.doi.org/10.1016/j.bmcl.2014.01.071.

References and notes

1. Berridge, M. J.; Lipp, P.; Bootman, M. D. *Nat. Rev. Mol. Cell Biol.* **2000**, *1*, 11.
2. Berridge, M. J.; Bootman, M. D.; Roderick, H. L. *Nat. Rev. Mol. Cell Biol.* **2003**, *4*, 517.
3. Santoni, G.; Santoni, M.; Nabissi, M. *Br. J. Pharmacol.* **2012**, *166*, 1244.
4. Zhang, Y.; Zhang, J.; Jiang, D.; Zhang, D.; Qian, Z.; Liu, C.; Tao, J. *Br. J. Pharmacol.* **2012**, *166*, 1247.
5. Gray, L. S.; Perez-Reyes, E.; Gamorra, J. C.; Haverstick, D. M.; Shattock, M.; McLatchie, L.; Harper, J.; Brooks, G.; Heady, T.; Macdonald, T. L. *Cell Calcium* **2004**, *36*, 489.
6. Lory, P.; Bidaud, I.; Chemin, J. *Cell Calcium* **2006**, *40*, 135.
7. (a) Berridge, M. J. *Neuron* **1988**, *21*, 13; (b) Yunker, A. M.; McEnery, M. W. *J. Bioenerg. Biomembr.* **2003**, *35*, 533.
8. Monteil, A.; Chemin, J.; Leuranguer, V.; Altier, C.; Mennessier, G.; Bourinet, E.; Lory, P.; Nargeot, J. *J. Biol. Chem.* **2000**, *275*, 16530.
9. Chemin, J.; Monteil, A.; Lory, P. *J. Soc. Biol.* **2003**, *197*, 235.
10. Perez-Reyes, E.; Lory, P. *CNS Neurol. Disord.: Drug Targets* **2006**, *5*, 605.
11. Perez-Reyes, E. *Physiol. Rev.* **2003**, *83*, 117.
12. Li, M.; Xiong, Z.-G. *Int. J. Physiol. Pathophysiol. Pharmacol.* **2011**, *3*, 156.
13. Latour, I.; Louw, D. F.; Beedle, A. M.; Hamid, J.; Sutherland, G. R.; Zamponi, G. W. *Glia* **2004**, *48*, 112.
14. Taylor, J. T.; Zeng, X.-B.; Pottle, J. E.; Lee, K.; Wang, A. R.; Yi, S. G.; Scruggs, J. A.; Sikka, S. S.; Li, M. *World J. Gastroenterol.* **2008**, *14*, 4984.
15. Li, W.; Zhang, S.-L.; Wang, N.; Zhang, B.-B.; Li, M. *Cancer Invest.* **2011**, *29*, 339.
16. Smith, R. A.; Brooks, D.; Cokkinides, V.; Saslow, D.; Brawley, O. W. *CA Cancer J. Clin.* **2013**, *63*, 88.
17. Heo, J. H.; Seo, H. N.; Choe, Y. J.; Kim, S.; Oh, C. R.; Kim, Y. D.; Rhim, H.; Choo, D. J.; Kim, J.; Lee, J. Y. *Bioorg. Med. Chem. Lett.* **2008**, *18*, 3899.
18. Jung, S. Y.; Lee, S. H.; Kang, H. B.; Park, H. A.; Chang, S. K.; Kim, J.; Choo, D. J.; Oh, C. R.; Kim, Y. D.; Seo, J. H.; Lee, K.-T.; Lee, J. Y. *Bioorg. Med. Chem. Lett.* **2010**, *20*, 6633.
19. Kang, H. B.; Rim, H. K.; Park, J. Y.; Choi, H. W.; Choi, D. L.; Seo, J. H.; Chung, K. S.; Huh, G.; Kim, J.; Choo, D. J.; Lee, K.-T.; Lee, J. Y. *Bioorg. Med. Chem. Lett.* **2012**, *22*, 1198.
20. Rim, H. K.; Lee, H. W.; Choi, I. S.; Park, J. Y.; Choi, H. W.; Choi, J. H.; Cho, Y. W.; Lee, J. Y.; Lee, K.-T. *Bioorg. Med. Chem. Lett.* **2012**, *22*, 7123.
21. Shu, Y.-Z.; Johnson, B. M.; Yang, T. J. *AAPS J.* **2008**, *10*, 178. and references therein.
22. Monteil, A.; Chemin, J.; Bourinet, E.; Mennessier, G.; Lory, P.; Nargeot, J. *J. Biol. Chem.* **2000**, *275*, 6090.
23. Rubinstein, L.V.; Shoemaker, R. H.; Paull, K. D.; Simon, R. M.; Tosini, S.; Skehan, P.; Scudiero, D. A.; Monks, A.; Boyd, M. R. *J. Natl. Cancer Inst*. **1990**, *82*, 1113: The effect of synthetic compound on cell viability was assessed by using the 3-(4,5-dimethylthiazol-2-yl)-2,5-diphenyltetrazolium bromide (MTT) assay in 3 replicates. Each cancer cells were seeded and incubated in 96-well, flat-bottomed plates for 24 h and were exposed to various concentrations of test agents dissolved in DMSO (final concentration, 0.1%) for 48 h. Controls received DMSO vehicle at a concentration equal to that in drug-treated cells. The medium was removed, replaced by 200 μL of 0.5 mg/mL MTT in 10% fetal bovine serum containing RPMI, and cells were incubated in the carbon dioxide incubator at 37 °C for 2 h. Supernatants were removed from the wells and the reduced MTT dye was solubilized in 100 μL/well DMSO. Absorbance at 540 nm was determined on a plate reader.
24. Lee, K. W.; Kim, H. J.; Lee, Y. S.; Park, H. J.; Choi, J. W.; Ha, J.; Lee, K.-T. *Carcinogenesis,* **2007**, *28*, 1928: A549 cells were treated with 5 μM concentrations of each compound, washed with 1 mL phosphate buffered saline (PBS), fixed in 70% ice-cold ethanol, and kept in a freezer overnight. The fixed cells were centrifuged, washed twice with PBS and re-suspended in PBS containing 50 mg/mL PI and 100 μg/mL DNase-free RNase A. The cell suspension, which was hidden from light, was incubated for 30 min and analyzed using the fluorescence-activated cell sorting cater-plus FACS (Becton Dickinson Co, Heidelberg, Germany). Raw data for the distribution of DNA content were expressed as the percentage of cells in the sub-G_1, G_0/G_1, S, and G_2/M populations.
25. Hwang, J. A.; Hwang, M. K.; Jang, Y.; Lee, E. J.; Kim, J. E.; Oh, M. H.; Shin, D. J.; Lim, S.; Ji, G. O.; Oh, U.; Bode, A. M.; Dong, Z.; Lee, K. W.; Lee, H. J. *J. Nutr. Biochem.* **2013**, *24*, 1096.
26. Kondratskyi, A.; Yassine, M.; Kondratska, K.; Skryma, R.; Slomianny, C.; Prevarskaya, N. *Front Physiol.* **2013**, *4*, 272.
27. Miri, R.; Motamedi, R.; Rezaei, M. R.; Firuzi, O.; Javidnia, A.; Shafiee, A. *Arch. Pharm.* **2011**, *344*, 111.
28. Giordanetto, F.; Knerr, L.; Selmi, N.; Llinàs, A.; Lindqvist, A.; Wang, Q.-D.; Ståhlberg, P.; Thorstensson, F.; Ullah, V.; Nilsson, K.; O'Mahony, G.; Högberg, Å.; Lindhardt, E.; Åstrand, A.; Duker, G. *Bioorg. Med. Chem. Lett.* **2011**, *21*, 5557.
29. Ki, Y. S.; Park, E.Y.; Lee, H. W.; Oh, M. S.; Cho, Y. W.; Kwon, Y. K.; Moon, J. H.; Lee K.-T. *Biol. Pharm. Bull*. **2010**, *33*, 1054: For PI and Annexin V double staining, A549 cells were suspended with 100 μL of binding buffer (10 mM HEPES/NaOH, 140 mM NaCl, 2.5 mM $CaCl_2$, pH 7.4) and stained with 5 μL of FITC-conjugated Annexin V and 5 μL of PI (50 μg/mL) for 15 min at room temperature in dark place and then added 400 μL binding buffer, and analyzed by the fluorescence-activated cell sorting (FACS) cater-plus flow cytometry (Becton Dickinson Co, Heidelberg, Germany).
30. Thornberry, N. A.; Lazebnik, Y. *Science* **1998**, *281*, 1312.
31. Nagata, S. *Cell* **1997**, *88*, 355.
32. Nicholson, D. W. *Cell Death Differ.* **1999**, *6*, 1028.
33. Earnshaw, W. C.; Martins, L. M.; Kaufmann, S. H. *Annu. Rev. Biochem.* **1999**, *68*, 383.
34. Kaufmann, S. H.; Earnshaw, W. C. *Exp. Cell Res.* **2000**, *256*, 42.
35. Ashkenazi, A.; Dixit, V. M. *Science* **1998**, *281*, 1305.
36. Green, D. R.; Reed, J. C. *Science* **1998**, *281*, 1309.
37. Budihardjo, I.; Oliver, H.; Lutter, M.; Luo, X.; Wang, X. *Annu. Rev. Cell Dev. Biol.* **1999**, *15*, 269.
38. Mohamed, A. E.; Zhu, Q.; Wang, Q.; Gulzar, W.; Altaf, A. W. *Int. J. Cancer* **2005**, *117*, 409.
39. *The spectral data for* **6e** (**BK10040**: free form): mp 228–240 °C (salt); ^{1}H NMR (400 MHz, $CDCl_3$) δ 7.29–7.23 (3H, m, Ph), 7.22–7.16 (3H, m, Ph), 7.13–7.11 (1H, m, Ph), 7.06–6.99 (4H, m, Ph), 6.96–6.87 (2H, m, Ph), 5.81 (1H, t, J = 5.6 Hz, –CO–N*H*–CH_2–), 5.17 (1H, dd, J = 9.6 and 5.6 Hz, –CO–CH_2–CH–N–), 4.47–4.38 (2H, m, –NH–CH_2–Ph–), 3.32 (4H, m, –N–(CH_2–CH_2)$_2$–NCH_2–), 2.58 (1H, dd, J = 14.0 and 9.6 Hz, –CO–CH_2–), 2.42 (1H, dd, J = 14.0 and 9.6 Hz, –CO–CH_2–), 2.45–2.40 (1H, m, Ph-*cyclohexyl*), 2.34 (4H, s, –N–CH_2–CH_2–NMe_2), 2.22 (6H, s, –NMe_2), 2.17 (4H, m, –N–(CH_2–CH_2)$_2$–N–CH_2–), 1.83–1.81 (4H, m, cyclohexyl), 1.75–1.71 (1H, m, cyclohexyl), 1.39–1.32 (4H, m, cyclohexyl), 1.29–1.21 (1H, m, cyclohexyl); ^{13}C NMR (100 MHz, $CDCl_3$) δ 170.0, 153.4, 144.1, 143.6, 143.3, 138.0, 128.7, 128.2, 128.1, 127.6, 127.4, 126.3, 125.0, 122.6, 122.5, 122.5, 56.8, 56.6, 52.9, 45.9, 45.7, 43.9, 43.8, 42.2, 34.5, 34.4, 26.9, 26.1; HRMS (FAB+): m/z estimated for $C_{37}H_{49}N_6O$ $[M+H]^+$ 593.3968, found: 593.3969.